Nonlinear MHD Milestones 2007 Q2

1. Improve understanding of the present discrepancy between NIMROD and M3D and move to new CDX-U-relevant cases with more realistic parameters and sources.
Q2: M3D to understand q_0 evolution, and NIMROD to perform nonlinear calculation with several values of q_0 to determine dependence. (J. Breslau, C. Sovinec)
Report:

NIMROD has now rerun the CDX-U benchmark with two new equilibrium corresponding to q_0=0.82 and q_0=0.71. Both of these runs exhibit periodic sawtooth behavior and have been run for 3 sawtooth periods. The q_0=0.82 case was extensively converged both with respect to element order and to toroidal mode number, going up to n=21. The dimensionless linear growth rate was determined to be: $\gamma\tau_A=1.39\times10^{-2}$. This case was chosen to be compared in detail with M3D

After exhaustive testing in M3D, it was determined that the large and steady drop in q_0 over time in the 2D nonlinear case beginning from equilibrium was a consequence of a lack of good conservation properties in the formulation of the equation for C (toroidal current density) in the presence of large 2D flows and low resistivity when a current source term is used. (The large 2D flows had previously been established to result from equilibrium discretization errors in the interpolation of the VMEC equilibrium onto M3D's linear finite element mesh; the amplitude of the flow converges to zero as the M3D mesh resolution is increased, and the rate of change of q_0 drops proportionately). The C equation has now been reformulated to a more conservative form, in which the derivative of the right-hand-side is taken numerically rather than algebraically. As a result, the rate of change of q_0 in the 2D case is reduced to insignificance. A full 3D nonlinear calculation performed using the new C equation confirms that q_0 and the n=1 growth rate now both remain constant until well into the nonlinear regime. The q_0=0.82 case gave a converged growth rate of $\gamma\tau_A=1.7\times10^{-2}$ which is in reasonable agreement with the NIMROD result on this equilibrium. But more significantly, the nonlinear M3D and NIMROD results for the q_0 =0.82 case are now in much better qualitative and quantitative agreement. These results are detailed in the appendices of this report.

2. Perform a linear edge stability calculation in a non-diverted equilibrium with a resistive code, and compare results with the linear ideal MHD code ELITE.
Q2: Perform scans of resistivity values and profiles to study how the resistive, linear MHD results converge to the ideal MHD results for each toroidal mode number with an equilibrium that is robustly unstable peeling-ballooning modes. (S. Kruger, P. Snyder)
Report:

Prior experience of benchmarking ELITE, GATO, and DCON has shown that difference in equilibrium mapping can account for ~5-10% differences in growth rates, and that when an inverse equilibrium is used, the differences were reduced to less than 2%. For this reason, our goal was to try and use an inverse solver such as TOQ. The difficulty

with this approach is that NIMROD requires a Grad-Shafranov solution in the vacuum region. The solution was to modify TOQ to solve for the vacuum region as well, which is possible for weakly-shaped cross sections. Another numerical difficulty is that NIMROD must transition from a low resistivity plasma to a high resistivity plasma over a narrow region. To minimize the influence of the resistive transition region on the NIMROD growth rates, we are choosing an equilibrium that has a wider pedestal width than those normally studied.

We have successfully created an equilibrium that has the parameters we desire. Its features can be seen in Figure 1. The pressure profile is flat in the core to avoid pressure-driven core instabilities. The current at the edge includes the self-consistent bootstrap current using the Sauter model. The pedestal width given is approximately 10% of the normalized poloidal flux, which is approximately twice the normal experimental width. The vacuum region can be discerned from examining the pressure profile versus major radius at the midplane. Because of how this equilibrium is constructed there is a large Shafranov shift. On the outboard midplane, there is approximately 40 cm of vacuum region versus a minor radius of approximately 85 cm.

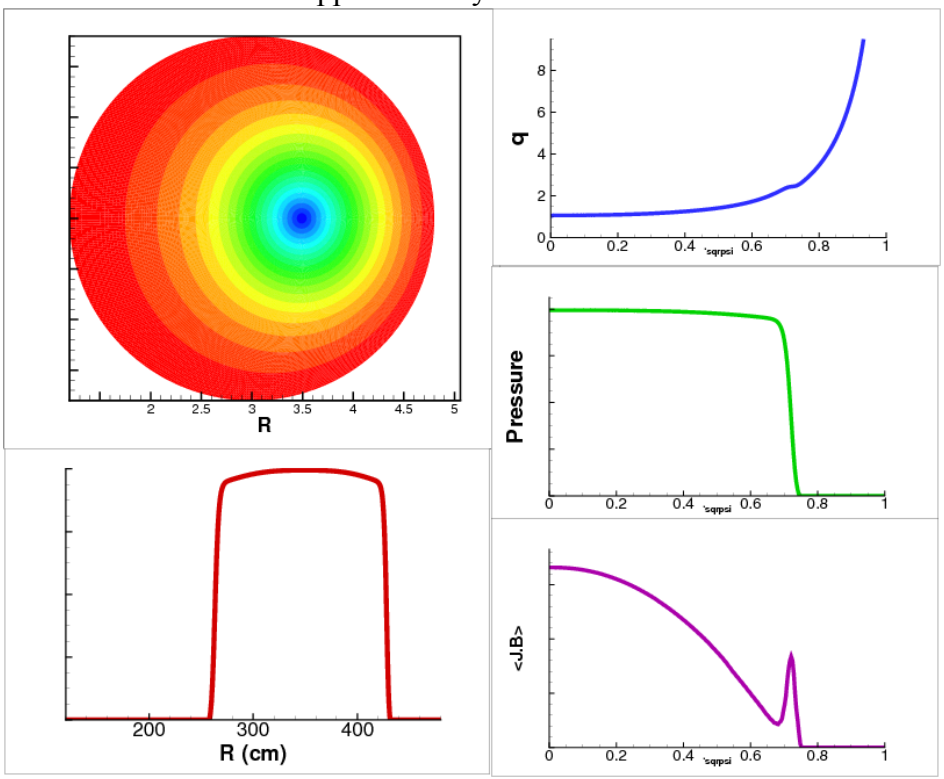

Figure 1. Equilibrium (labeled krmb1) designed for benchmark studies shows characteristics of H-mode plasmas while simplifying core profiles and geometry for benchmark purposes. It was generated with the TOQ equilibrium solver.

As expected, GATO and ELITE give excellent agreement with the equilibrium as shown in Figure 2. The unique growth rate spectrum is due to the rational q's which are near the surface, and is indicative of a strong peeling component in this case. GATO was run with and without a wall at $r_{wall}/a=1.8$ to give an indication of the importance of wall stabilization. For this equilibrium, the wall is a relatively unimportant effect.

Simulations have begun by both the NIMROD and M3D teams, but no results are available at this time.

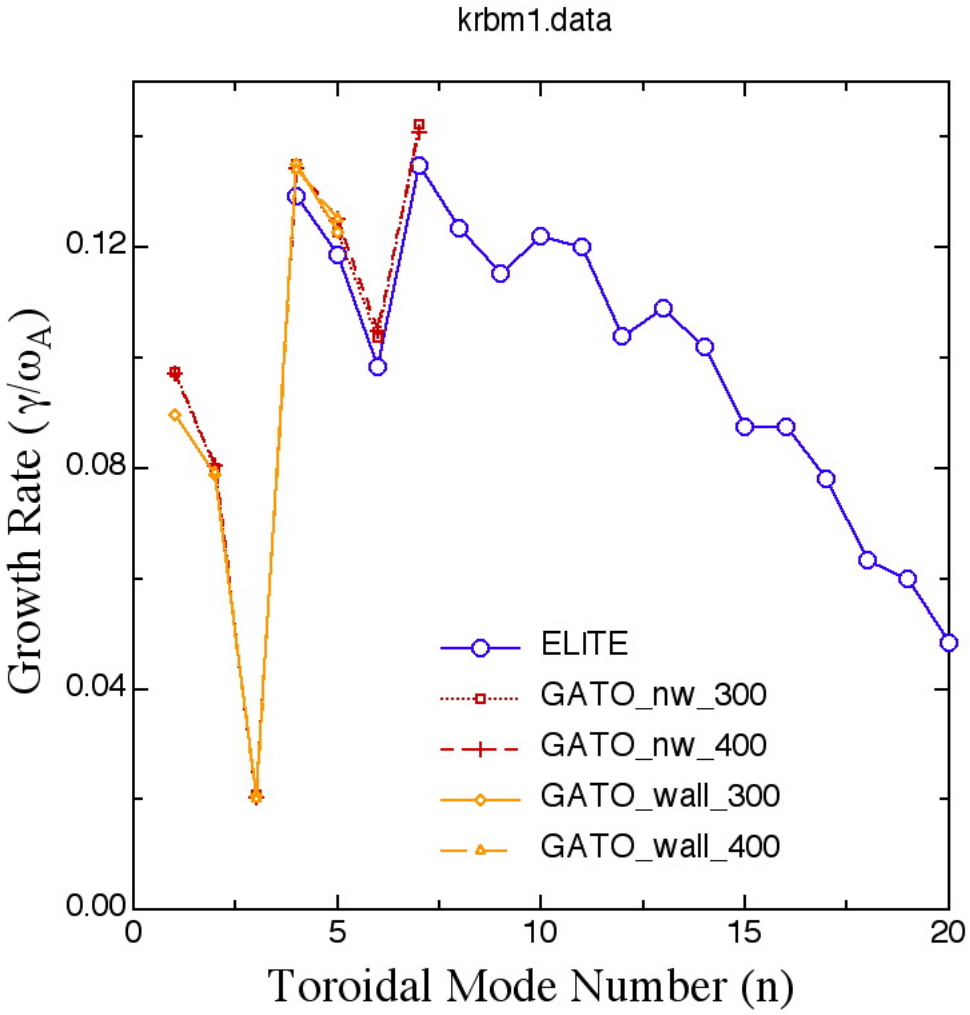

3. Extend the 2D GEM nonlinear benchmark to non-zero guide field and more extreme parameters.
Q2: Perform exploratory studies of non-zero guide field case and better define parameters. (S. Jardin)

Report:
What has become a "standard problem" in 2-fluid magnetic reconnection was proposed in [J. Birn, J. F. Drake, M. A. Shay, *et al.*, J. Geophys. Res., [Space Phys.] **106**, 3715 (2001)]. In there, they define initial values for the equilibrium poloidal flux, in-plane magnetic field, total pressure, density, and electron pressure as follows;

$$\psi^0(x,y) = \frac{1}{2}\ln\left(\cosh 2y\right)$$
$$B_z^0(x,y) = 0$$
$$P^0(x,y) = \frac{1}{2}\left[\sec h^2(2y) + 0.2\right]$$
$$n^0(x,y) = \left[\sec h^2(2y) + 0.2\right]$$
$$P_e^0(x,y) = 0.2P^0(x,y)$$

All other quantities are initialized to zero. A perturbation is applied at time *t=0* as follows:

$$\psi(x,y) = \varepsilon \cos k_x x \cos k_y y\ .$$

The initial equilibrium and perturbed current densities are just the Laplacian of the fluxes, $J^0 = -\nabla^2\psi^0, J = -\nabla^2\psi$. The computation is carried out in a rectangular domain: $-L_x/2 \le x \le L_x/2$ and $-L_y/2 \le y \le L_y/2$. The system is taken to be periodic in the *x*-direction with ideal conducting boundaries at $y = \pm L_y/2$. The parameters are chosen such that $k_x = 2\pi/L_x$, $k_y = \pi/L_y$, with $L_x = 25.6, L_y = 12.8,$ and $\varepsilon = 0.1$. These calculations used values of resistivity η = *0.005*, viscosities $\mu=\mu_C$=*0.05*, and thermal conductivity κ=*0.02*.

Since the current could be carried by either the electrons or the ions, there is another degree of freedom in specifying the initial equilibrium. Thus, we have introduced the variable $f_i \equiv$ VELION which is the fraction of the initial toroidal current that is carried by the ions. Thus, in general we define an initial ion velocity:

$$V_z^0 = -f_i \frac{1}{n}\nabla^2\psi^0$$

Another variable we introduced was the fraction of the initial pressure profile that was due to density variation as opposed to temperature variation. Thus, we introduce another variable $f_n \equiv$ FACDEN into the equilibrium definition as follows:

$$n^0(x,y) = \left[\ f_n \sec h^2(2y) + 0.2\right]$$

We have experimented with varying f_i in the range 0-1, and f_n in the range 0.1 to 1, and the viscosity in the range 0.05 to 0.005. We find that as f_n is lowered from 1, the fast reconnection becomes more pronounced, as it does when the viscosity is lowered from .05 to .005. Both of these also make the resolution requirements more severe.

In order not to exacerbate the severe resolution requirements, and to aid in direct comparison with the zero-guide field studies, we are thus recommending that at this stage that we keep the same profiles with $f_i = 0$ (all equilibrium currents are carried by the electrons) and $f_n = 1$ (same equilibrium density profile as in GEM), and the viscosity and thermal conductivity equal to .05 as they were in the GEM benchmark.

4. Scalability studies on leading edge computers:
Q2: Perform scaling studies of NIMROD on Jaguar, and identify bottlenecks.(E. Held)
Report:
One avenue toward scaling plasma fluid codes to tens of thousands of processors involves coupling codes such as NIMROD and M3D to kinetic calculations of closures. For example, the implementation of parallel closures in NIMROD requires on the order of 10^6 solutions to lowest-order, Chapman-Enskog-like (CEL), drift kinetic equations for every advance of the fluid equations.

We have completed the programming aspects of having one group of processors perform NIMROD's CEL parallel closure calculation while a separate group of processors advances the fluid equations. This required forming multiple communicator groups using the MPI split command so that processors treating different aspects of the problem (fluid versus kinetic) could easily communicate in their distinct groups as well as between the fluid and kinetic groups. Testing and debugging were completed on Bassi at NERSC. Due to the present revamping of Jaguar at ORNL (it is down while new processors are being added), the code is presently being ported to Seaborg for scaling studies up to at least 4000 processors. Once Jaguar is up and running again, scaling studies will be performed there as well. Preliminary calculations are encouraging and suggest that in addition to adding important physics to the fluid model, the massively parallel calculation of closures is a viable avenue toward running plasma fluid codes on thousands of processors.

Appendix I: Nonlinear NIMROD Results on the CDXU q(0)=0.82 Case

Carl Sovinec

March 1, 2007

A pair of nonlinear simulations for the CDXU equilibrium with $q(0)$=0.82 has been run with NIMROD. The physical parameters for the computations are listed in Table I and have been selected to match the dimensionless parameters used for the $q(0)$=0.92 case. The major radius is 0.3754 m, and the minor radius is 0.2409 m. The dimensional Alfvén time is slightly smaller than the previous case, because $B_\phi(0)$ is slightly larger (0.1359 T; 0.1315 T for the larger-q_0 case). The computations have been run with a 40×60 mesh of biquadratic elements that conform to the equilibrium flux surfaces. Linear tests with the same mesh, physical parameters, and either biquadratic or bicubic elements show that the 1/1 mode grows at $\gamma\tau_A=1.39\times10^{-2}$. The nonlinear computations are initialized with the 1/1 eigenmode only, as specified for the benchmark. The finite Fourier series in the first of the two nonlinear computations has 0≤n≤10, and it has 0≤n≤21 in the second. The computations use NIMROD's separate steady-state capability, which is equivalent to having sources that maintain the equilibrium profile against dissipation.

The evolution of the kinetic fluctuation spectrum (Fig. 1) shows repeating 1/1 activity, but only the high-n modes 'crash' after each event. The n=1 itself decays with a rate that has roughly the same value as its growth rate when it is increasing. The activity appears to damp very slight with each event, so it is not clear whether the cycle will repeat indefinitely. The results are not sensitive to toroidal resolution. The comparison provided in Fig. 1 shows that the 0≤n≤10 case is already well resolved.

Table I. Parameters used for the CDX-U benchmark with $q(0)$=0.82.

quantity	NIMROD (dimensional)	dimensionless
Z_{eff}	2	2
$n_e(0)$	1.374×10^{19} m^{-3}	-
$\rho(0)$	1.149×10^{-8} kg/m^3	1
m_i	1.673×10^{-27} kg	-
τ_A	3.319×10^{-7} s	1
$\eta(0)/\mu_0$	9.005 m^2/s	5.15×10^{-5}
τ_r	6.445×10^{-3} s	1.94×10^{4}
$D_{particle}$	174.9 m^2/s	1×10^{-3}
$\nu_{kinematic}$	90.05 m^2/s	5.15×10^{-4}
χ_{perp}*	158.9 m^2/s	9.09×10^{-4}
$\chi_{parallel}$*	1.0×10^{8} m^2/s	572.

*The thermal diffusivities are NIMROD input values. The actual thermal diffusivities are 3/2 larger.

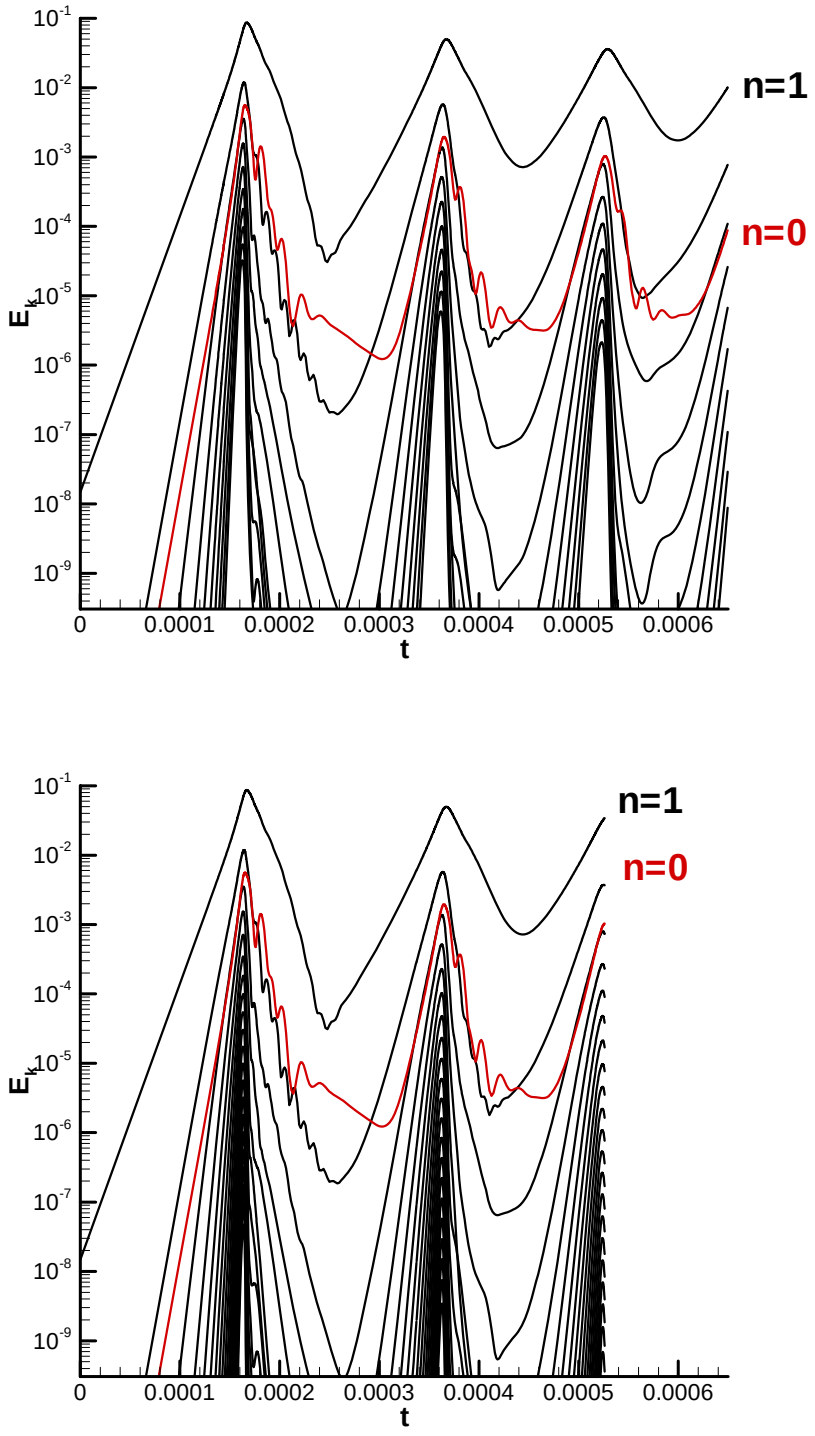

Figure 1. Temporal evolution of kinetic energy in each toroidal harmonic vs. time from NIMROD simulations with $0 \le n \le 10$ (top) and with $0 \le n \le 21$ (bottom).

The remaining plots show the changes in magnetic topology and its effect on the temperature distribution during the first event in the second simulation. Figure 2 is a Poincaré plot of the magnetic field during the initial growth of the mode. Figure 3 shows a set of Poincaré plots starting from the time when the high-n activity peaks (the magnetic energy in the n=1 mode is already decreasing slightly at this time). The final plot in the sequence is still before the fluctuation energy reaches a minimum, but the flux surfaces have largely returned.

The maximum electron temperature at the start of the computation is 101.5 eV. At the time of peak high-n activity (163 μs), the temperature drops to 80.7 eV. It regains as the flux surfaces return, reaching 95.7 eV at 200 μs. However, it should be noted that the heating is from the effective thermal energy source and not a realistic Ohmic heating with temperature-dependent resistivity. Finally, Table II compares peak temperatures from the two nonlinear simulations from data files that are as closely matched in time as possible.

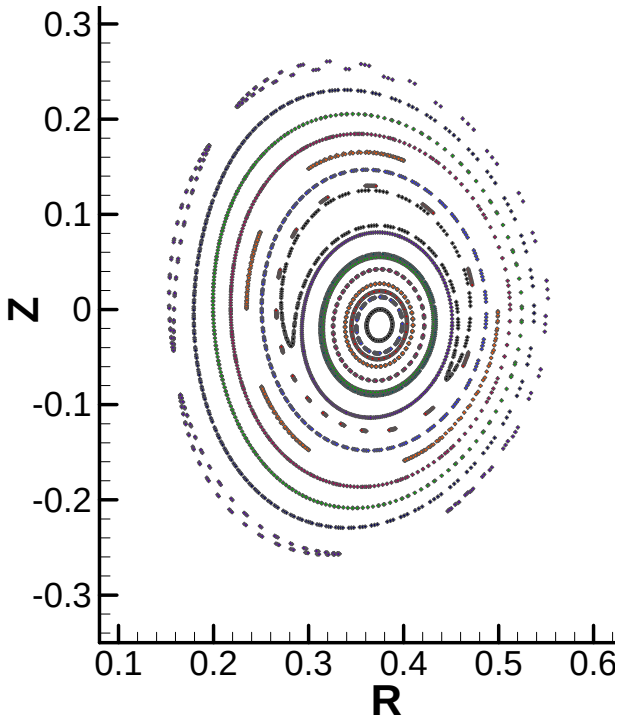

Figure 2. Poincaré surface of section at ϕ=0 and t=129 μs into the computation with 0≤n≤21.

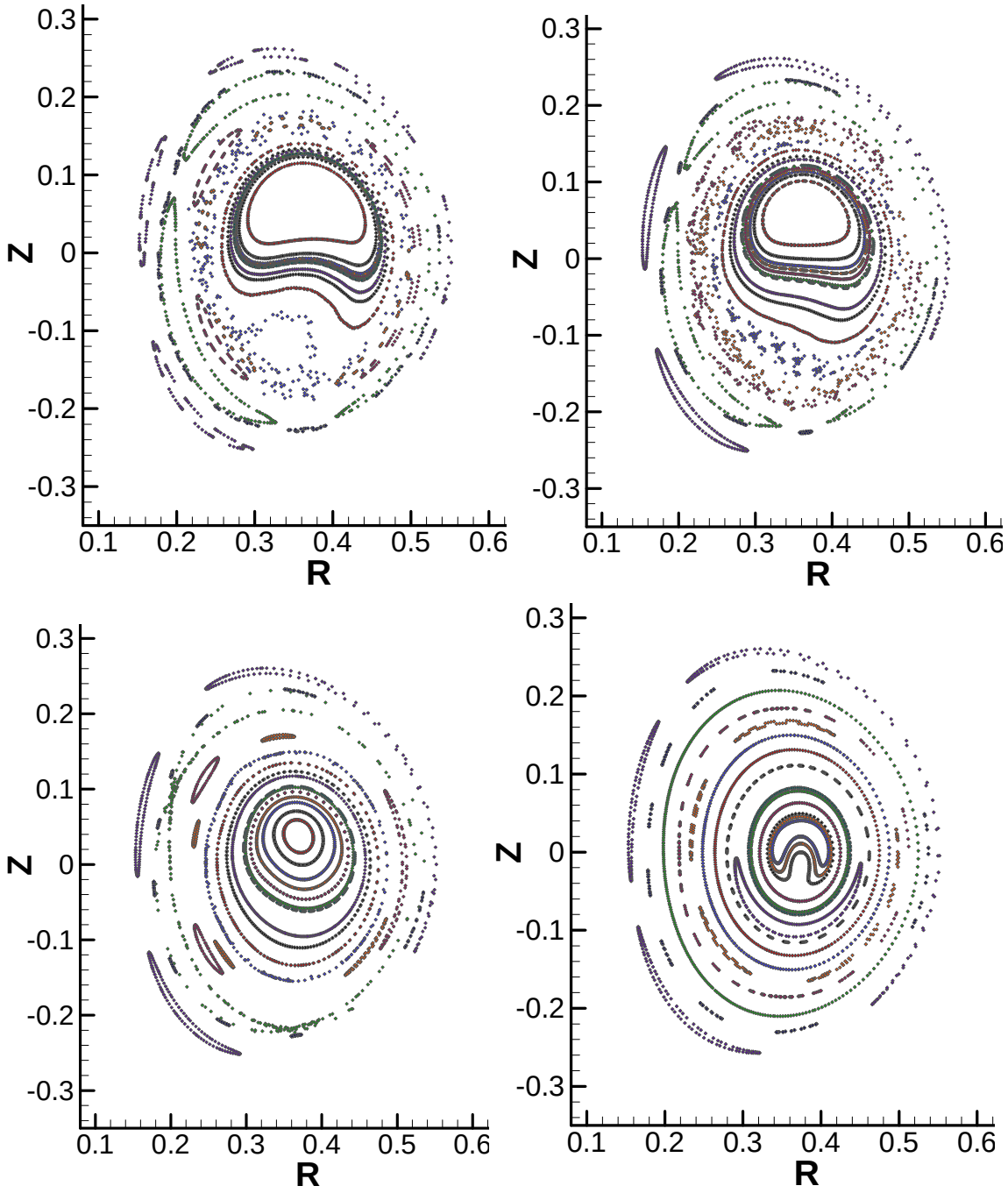

Figure 3. Poincaré surfaces of section at ϕ=0 and t=163 μs (top left), 166 μs (top right), 172 μs (lower left), and 200 μs (lower right) into the computation with 0≤n≤21.

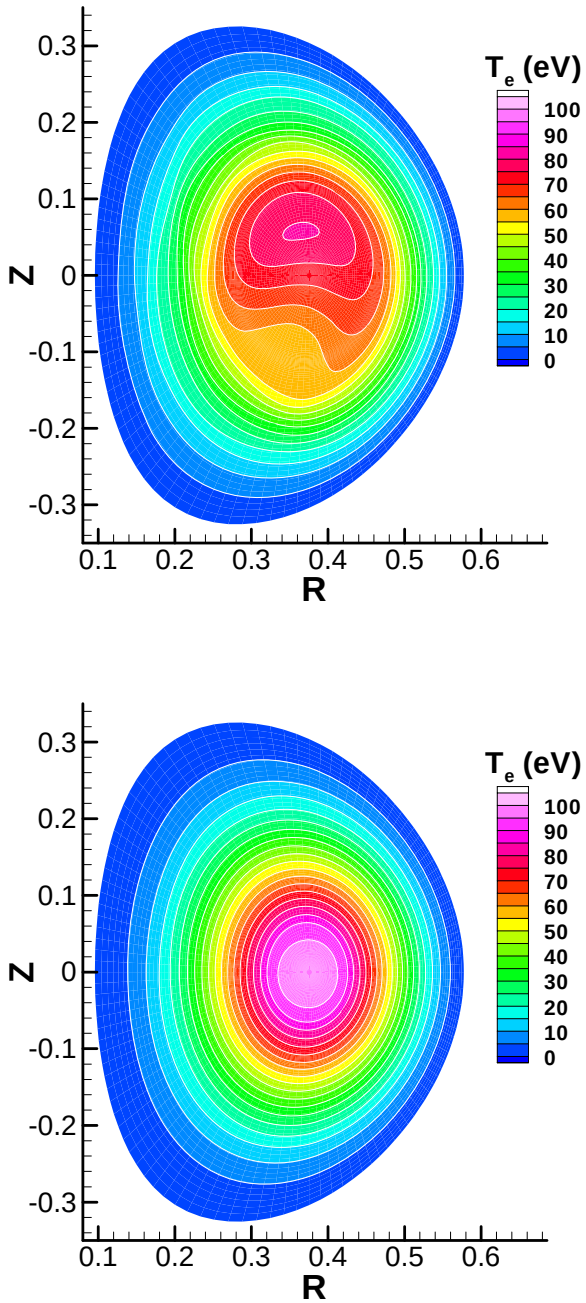

Figure 4. Temperature profiles at ϕ=0 and t=163 μs (left) and 200 μs (right) from the computation with 0≤n≤21.

Table II. Comparison of results on peak temperature for the two simulations.

0≤n≤10	0≤n≤21

t (μs)	T_e (eV)	t (μs)	T_e (eV)
0	101.5	0	101.5
128	101.3	129	101.0
163	80.9	163	80.7
166	84.4	166	84.3
172	89.9	172	89.9
218	97.6	200	95.7

Appendix II: Nonlinear NIMROD Results on the CDXU q(0)=0.71 Case

Carl Sovinec

March 20, 2007

- Equilibrium label: run06time29
- Physical parameters: see Table I. Dimensionless parameters use a=0.2414 m.
- Numerical parameters: 40×60 mesh of biquadratic elements, 0≤n≤10 (no convergence testing
- Linear growth rate for the 1/1 mode: $\gamma\tau_A$=0.0226

Table I. Parameters used for the CDX-U benchmark with $q(0)$=0.71.

quantity	NIMROD (dimensional)	dimensionless
Z_{eff}	2	2
$n_e(0)$	1.374×10^{19} m^{-3}	-
$\rho(0)$	1.149×10^{-8} kg/m^3	1
m_i	1.673×10^{-27} kg	-
τ_A	3.212×10^{-7} s	1
$\eta(0)/\mu_0$	9.34 m^2/s	5.15×10^{-5}
τ_r	6.239×10^{-3} s	1.94×10^{4}
$D_{particle}$	181.4 m^2/s	1×10^{-3}
$\nu_{kinematic}$	93.4 m^2/s	5.15×10^{-4}
χ_{perp}*	164.8 m^2/s	9.09×10^{-4}
$\chi_{parallel}$*	1.0×10^{8} m^2/s	552.

*The thermal diffusivities are NIMROD input values. The actual thermal diffusivities are 3/2 larger.

Appendix III:

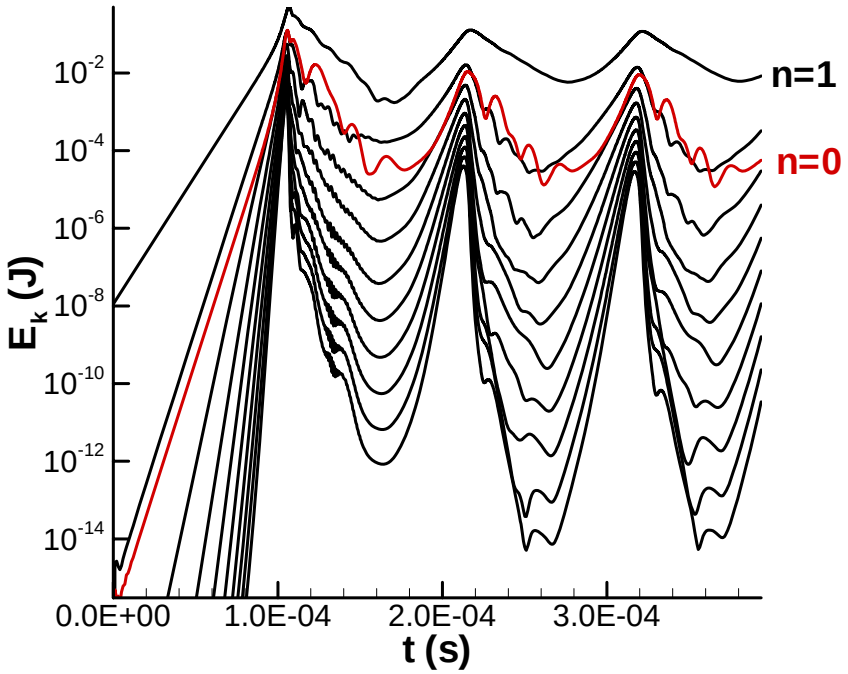

Figure 1. Temporal evolution of kinetic fluctuation energies.

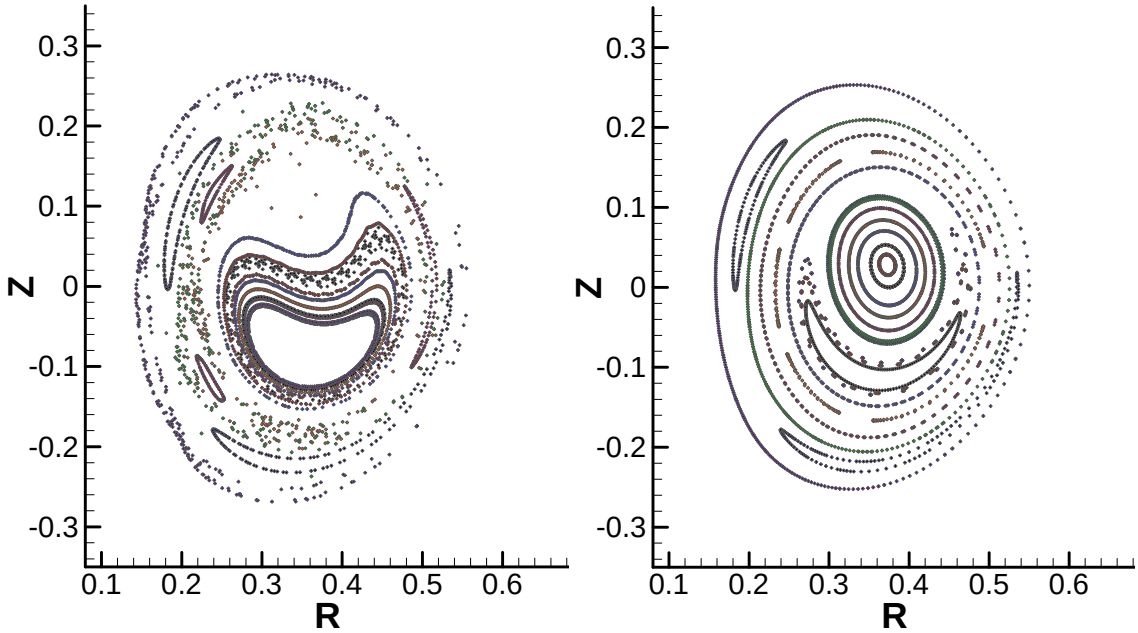

Figure 2. Poincaré surfaces of section for the ϕ=0 plane at t=317 μs (left) and at t=386 μs (right).

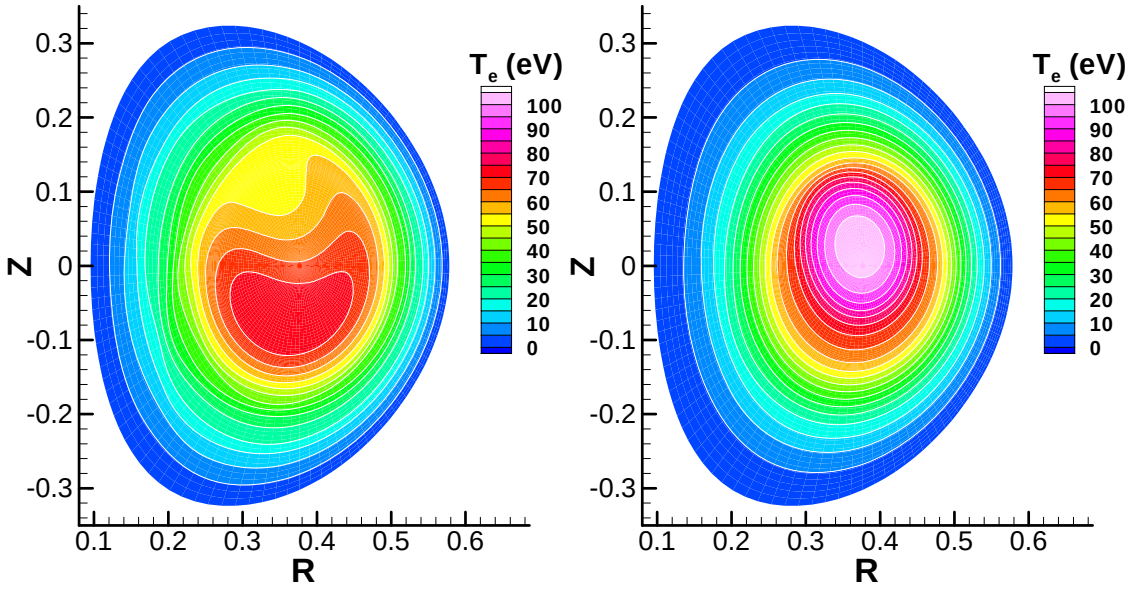

Figure 3. Contours of constant electron temperature for the ϕ=0 plane at t=317 μs (left) and at t=386 μs (right).

Table II. Estimated sawtooth period for the three CDXU computations with the dimensionless parameters listed in Table I.

	$q(0)$=0.71	$q(0)$=0.82	$q(0)$=0.92
Γ (μs)	100	160	270
Γ/τ_A	320	490	790

Appendix III: Nonlinear M3D Results on the CDX-U q(0)=0.82 Case

Josh Breslau

March 22, 2007

This case was run with the new, conservative form of the equation for C (toroidal current density), which does a much better job of maintaining the q profile in the n=0 piece. In order to isolate the effect of this change, the case was run at the same resolution and with the same parameters as the previous nonlinear M3D run: 24 planes (up to n=10); 79 radial zones, and 3 theta partitions. As before, I used the new isotropic viscosity and the same size time step (dt=0.004 τA), and did not use isotropic heat conduction. Other parameters are shown in the table.

The linear growth rate for the 1,1 mode at this resolution was found to be $\gamma\tau A \approx 1.63\times10$-2. Initial convergence tests did not show an easily identifiable power law convergence with mesh spacing, but the projected converged value is around 1.7 ×10-2.

To ease comparison of the nonlinear results with those from NIMROD, I have plotted the kinetic energies on a similar scale (with times converted to μs using Carl's value of 0.3319 μs for the Alfvén time). I started with a somewhat larger perturbation than before to save run time, but there is still a distinct linear regime in which the n=0 growth rate matches the linear rate without increasing before the nonlinearity sets in. I also terminated the run somewhat earlier than the NIMROD case. The large n=0 kinetic energy suggests that this case is not fully resolved poloidally.

For the Poincaré sections and temperature contours, I have chosen times and toroidal angles that seemed to correspond with those depicted in the NIMROD summary for ease of comparison. I am impressed with the level of agreement we now have between the codes.

Quantity	Value
η_0	5.15×10^{-5}(non-evolving Spitzer, cutoff=100)
ν	5.15×10^{-4}(constant isotropic)
$\kappa_\perp$	9.09×10^{-4}(perp to φ)
$\kappa_\parallel$	[Artificial sound speed = 6 V_A;$V_\mu=10^{-3}$
D_ρ	10^{-3}

Mode History

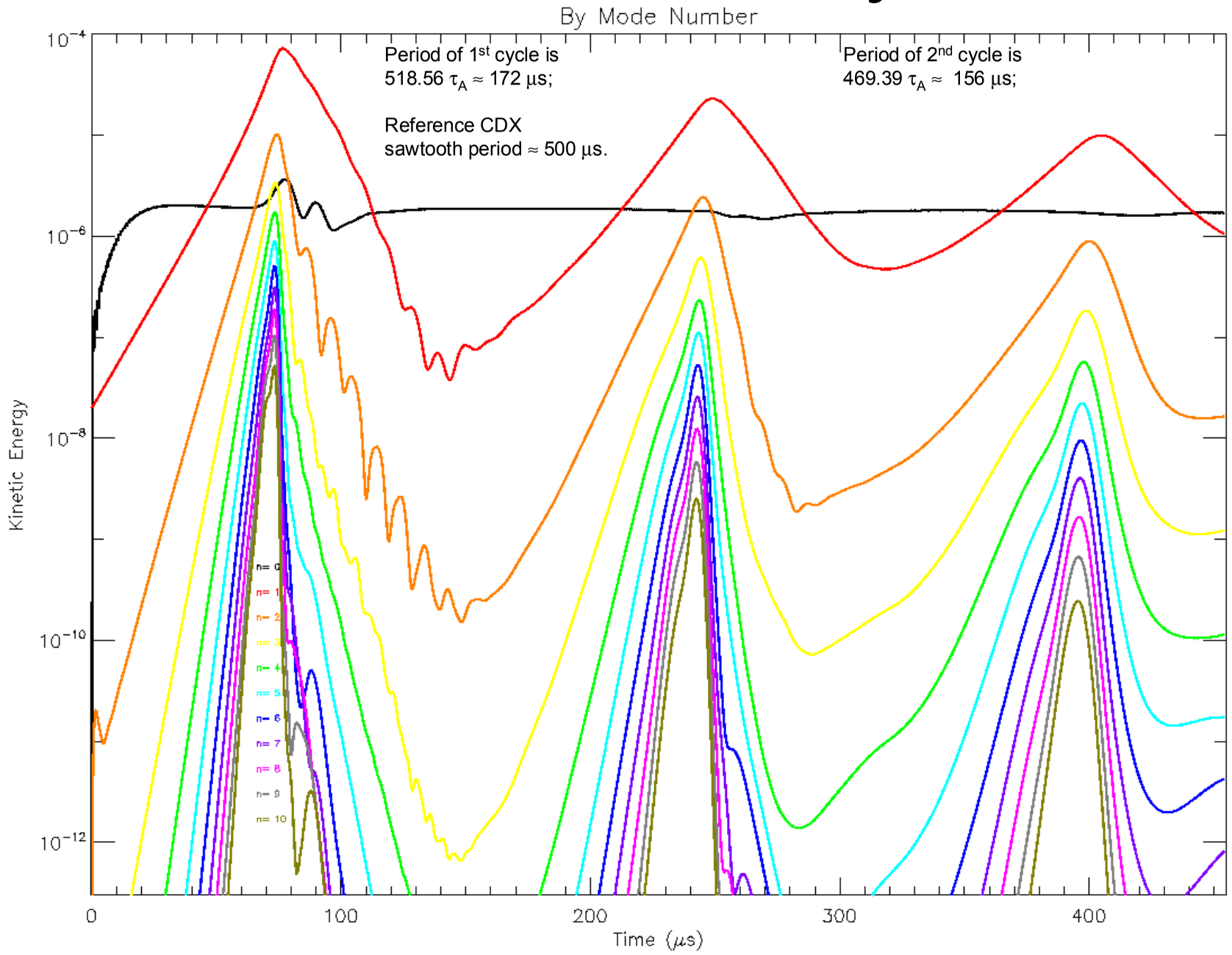

Poincaré Plots

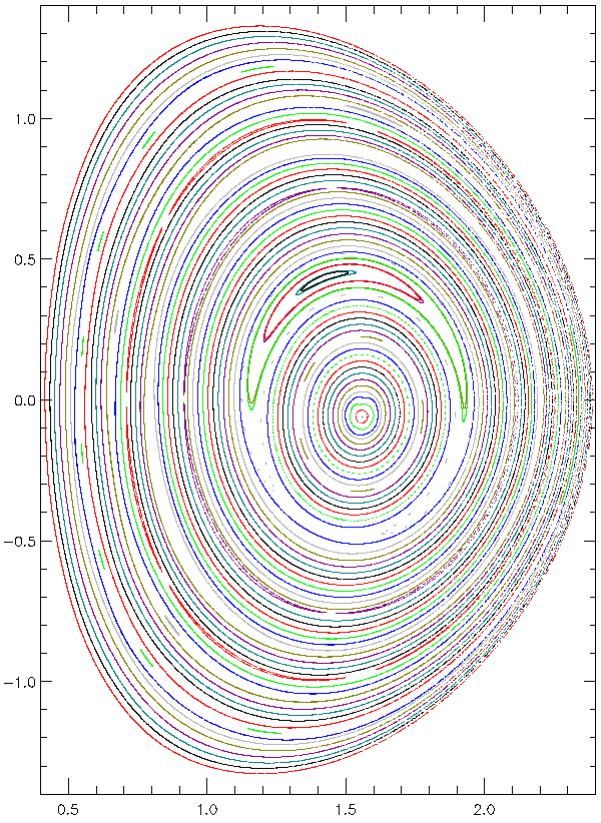

t = 38 μs; φ=π/2
(compare to NIMROD t=129 μs)

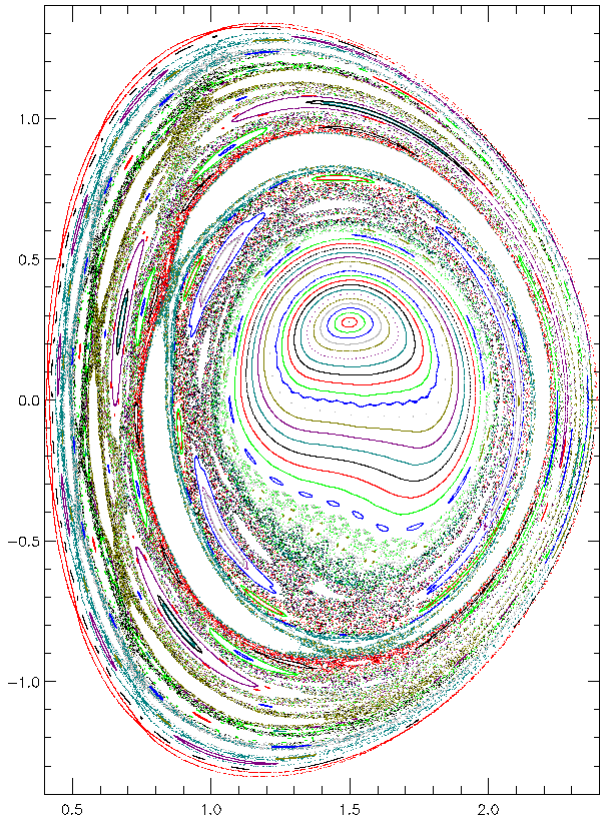

t = 75.5 μs; φ=π/2
(compare to NIMROD t=163 μs)

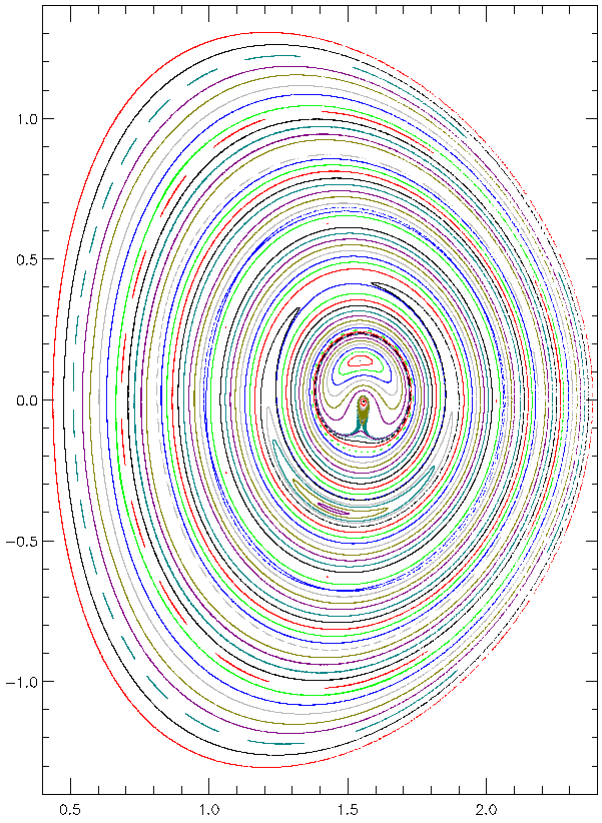

t = 115.3 μs; φ=π/2
(compare to NIMROD t=200 μs)

Temperature Contours

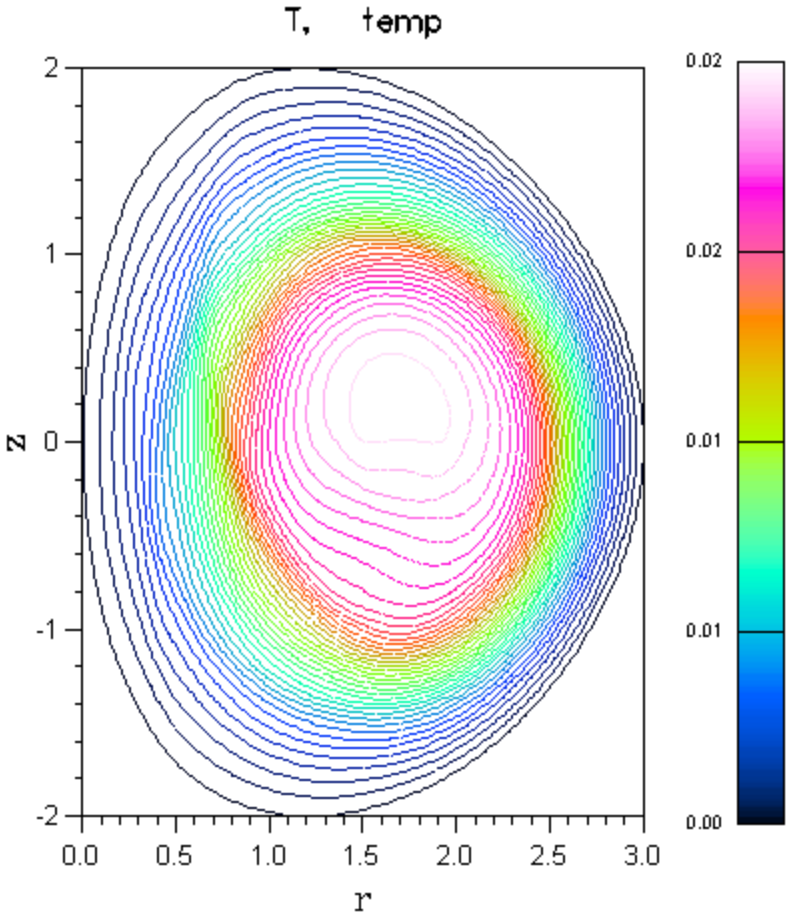

t = 75.5 μs; φ=π/2
(compare to NIMROD t=163 μs)

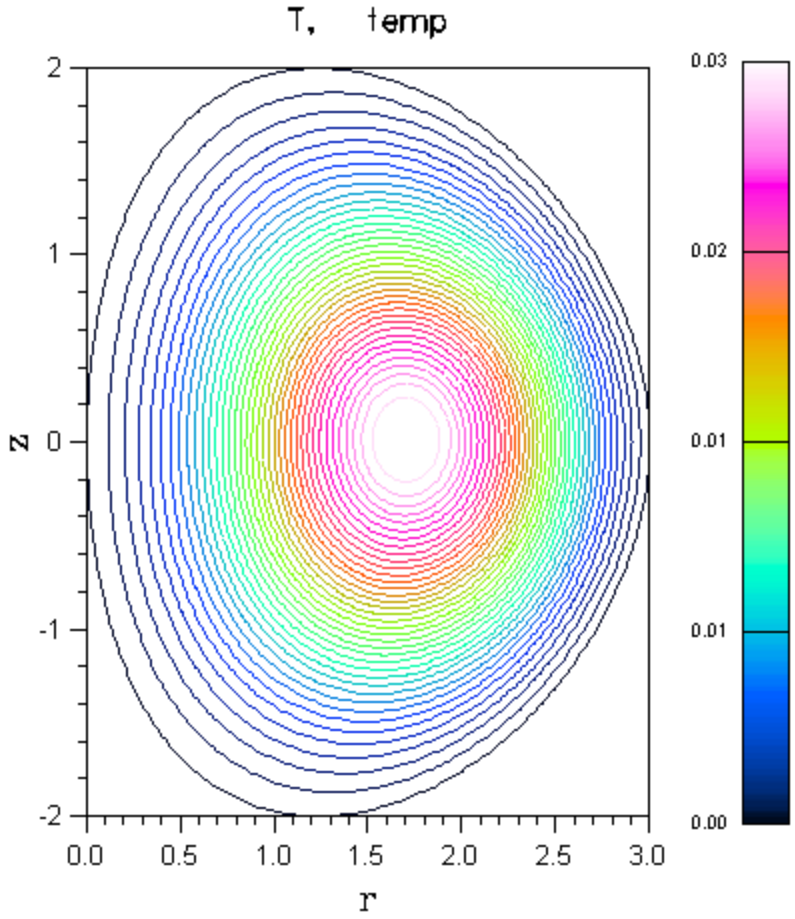

t = 115.3 μs; φ=π/2
(compare to NIMROD t=200 μs)